

Numerical approximation of nonlinear stochastic Volterra integral equation using Walsh function

Prit Pritam Paikaray^a, Nigam Chandra Parida^a, Sanghamitra Beuria^a, Omid Nikan^b

^aDepartment of Mathematics, College of Basic Science and Humanities, OUAT, Bhubaneswar, 751003, India

^bSchool of Mathematics and Computer Science, Iran University of Science and Technology, Narmak, Tehran, Iran

Abstract

This paper adopts a highly effective numerical approach for approximating non-linear stochastic Volterra integral equations (NLSVIEs) based on the operational matrices of the Walsh function and the collocation method. The method transforms the integral equation into a system of algebraic equations, which allows for the derivation of an approximate solution. Error analysis has been performed, confirming the effectiveness of the proposed method, which results in a linear order of convergence. Numerical examples are provided to illustrate the precision and effectiveness of this proposed method.

Keywords: Nonlinear stochastic Volterra integral equation, Itô integral, Brownian motion, Walsh approximation, Lipschitz condition, Collocation method.

2010 MSC: 60H05, 65C30

1. Introduction

Non-linear stochastic Volterra integral equations (NLSVIEs) have found various applications in the biological sciences, particularly in modeling and simulating biological systems. NLSVIEs have been used to model population growth and extinction in different species. For instance, they have been used to study the dynamics of predator-prey systems, where the population of predators and prey interact with each other in a non-linear way. NLSVIEs have been used to study the spread of infectious diseases in populations. In this case, the equations model the dynamics of the disease transmission, including the rate of infection and recovery, and the effect of different control measures. NLSVIEs have been used to model the dynamics of neuronal networks and synaptic plasticity in the brain. In this case, the equations model the non-linear interactions between neurons and how they change over time [1, 2]. However, it is impossible to obtain exact solutions for all NLSVIEs, various numerical techniques are adopted to obtain approximate solutions. In particular, numerical techniques including orthogonal functions are often applied to solve these problems. Haar wavelet [11], Orthogonal functions such as block pulse function (BPF) [9], and Legendre polynomials [10] have been implemented to simulate the solution of NLSVIEs. The Walsh function has also been employed for solving the stochastic Volterra integral equation [12].

In this work, we investigate the approximated solution $x(t)$ of the NLSVIE by using of the the Walsh

*Corresponding author

Email addresses: paikaraypritam@gmail.com (Prit Pritam Paikaray), ncparida@gmail.com (Nigam Chandra Parida), sbeuria108@gmail.com (Sanghamitra Beuria), omidnikan77@yahoo.com (Omid Nikan)

function [3] as

$$x(t) = x_0 + \int_0^t k_1(s, t)\beta(x(s))ds + \int_0^t k_2(s, t)\sigma(x(s))dB(s) \quad (1)$$

where $x(t)$ is an unknown function to be determined and $k_1(s, t)$, $k_2(s, t)$ for $s, t \in [0, T]$, represent the stochastic processes based on the same probability space (Ω, F, P) . Here $B(t)$ and $\int_0^t k_2(s, t)x(s)dB(s)$ denote the Brownian motion and Itô integral, respectively [1, 2].

The rest of current research paper is organized as follows. Section 2 introduces the Walsh Function and its properties. Section 3 describes Relationship between Walsh Function and Block Pulse Functions (BPFs). Section 4 presents a numerical technique by based on the operational matrices of the Walsh function and the collocation method to discretize the NLSVIEs. Section 5 discusses the convergence and error analysis of the method to demonstrate the method's validity and precision. Section 6 gives two numerical examples by using the proposed method to demonstrate the efficacy of the method. Finally, Section 7 contains some concluding remarks and summarizes the main findings.

2. Walsh Function and its Properties

Definition 1. Rademacher function $r_i(t)$, $i = 1, 2, \dots$, for $t \in [0, 1)$ is defined by [3]

$$r_i(t) = \begin{cases} 1 & i = 0, \\ \text{sgn}(\sin(2^i \pi t)) & \text{otherwise} \end{cases}$$

where,

$$\text{sgn}(x) = \begin{cases} 1 & x > 0, \\ 0 & x = 0, \\ -1 & x < 0. \end{cases}$$

Definition 2. The n^{th} Walsh function for $n = 0, 1, 2, \dots$, denoted by $w_n(t)$, $t \in [0, 1)$ is defined [3] as

$$w_n(t) = (r_q(t))^{b_q} \cdot (r_{q-1}(t))^{b_{q-1}} \cdot (r_{q-2}(t))^{b_{q-2}} \dots (r_1(t))^{b_1}$$

where $n = b_q 2^{q-1} + b_{q-1} 2^{q-2} + b_{q-2} 2^{q-3} + \dots + b_1 2^0$ is the binary expression of n . Therefore, q , the number of digits present in the binary expression of n is calculated by $q = \lceil \log_2 n \rceil + 1$ in which $\lceil \cdot \rceil$ is the greatest integer less than or equal's to \cdot .

The first m Walsh functions for $m \in \mathbb{N}$ can be written as an m -vector by $W(t) = [w_0(t) \ w_1(t) \ w_2(t) \ \dots \ w_{m-1}(t)]^T$, $t \in [0, 1)$. The Walsh functions satisfy the following properties.

Orthonormality

The set of Walsh functions is orthonormal. i.e.,

$$\int_0^1 w_i(t)w_j(t)dt = \begin{cases} 1 & i = j, \\ 0 & \text{otherwise.} \end{cases}$$

Completeness

For every $f \in L^2([0, 1))$

$$\int_0^1 f^2(t)dt = \sum_{i=0}^{\infty} f_i^2 \|w_i(t)\|^2$$

where $f_i = \int_0^1 f(t)w_i(t)dt$.

Walsh Function Approximation

Any real-valued function $f(t) \in L^2([0, 1])$ can be approximated as

$$f_m(t) \simeq \sum_{i=0}^{m-1} c_i w_i(t)$$

where, $c_i = \int_0^1 f(t) w_i(t) dt$.

The matrix form can be represented by

$$f(t) \simeq F^T T_W W(t) \quad (2)$$

where $F = [f_0 \ f_1 \ f_2 \ \dots \ f_{m-1}]^T$, $f_i = \int_{ih}^{(i+1)h} f(s) ds$.

Here, $T_W = [w_i(\eta_j)]$ is called as the Walsh operational matrix where $\eta_j \in [jh, (j+1)h)$.

Similarly, function $k(s, t) \in L^2([0, 1] \times [0, 1])$ can be approximated by

$$k_m(s, t) \simeq \sum_{i=0}^{m-1} \sum_{j=0}^{m-1} c_{ij} w_i(s) w_j(t)$$

where $c_{ij} = \int_0^1 \int_0^1 k(s, t) w_i(s) w_j(t) dt ds$ with the matrix form represented by

$$k(s, t) \simeq W^T(s) T_W K T_W W(t) = W^T(t) T_W K^T T_W W(s) \quad (3)$$

where $K = [k_{ij}]_{m \times m}$, $k_{ij} = \int_{ih}^{(i+1)h} \int_{jh}^{(j+1)h} k(s, t) dt ds$.

3. Relationship between Walsh Function and Block Pulse Functions (BPFs)

Definition 3. [Block Pulse Functions] For a fixed positive integer m , an m -set of BPFs $\phi_i(t)$, $t \in [0, 1)$ for $i = 0, 1, \dots, m-1$ is defined as

$$\phi_i(t) = \begin{cases} 1 & \text{if } \frac{i}{m} \leq t < \frac{(i+1)}{m}, \\ 0 & \text{otherwise} \end{cases}$$

in which ϕ_i is known as the i th BPF.

The set of all m BPFs can be written concisely as an m -vector, $\Phi(t) = [\phi_0(t) \ \phi_1(t) \ \phi_2(t) \ \dots \ \phi_{m-1}(t)]^T$, $t \in [0, 1)$. The BPFs are disjoint, complete, and orthogonal [4]. The BPFs in vector form satisfy

$$\Phi(t) \Phi(t)^T X = \tilde{X} \Phi(t) \text{ and } \Phi^T(t) A \Phi(t) = \hat{A} \Phi(t)$$

where $X \in \mathbb{R}^{m \times 1}$, \tilde{X} is the $m \times m$ diagonal matrix with $\tilde{X}(i, i) = X(i)$ for $i = 1, 2, 3 \dots m$, $A \in \mathbb{R}^{m \times m}$ and $\hat{A} = [a_{11} \ a_{22} \ \dots \ a_{mm}]^T$ is the m -vector with elements equal to the diagonal entries of A . The integration of BPF vector $\Phi(t)$, $t \in [0, 1)$ can be performed by [5]

$$\int_0^t \Phi(\tau) d\tau = P \Phi(t), t \in [0, 1), \quad (4)$$

Consequently, the integral of every function $f(t) \in L^2[0, 1)$ can be estimated as

$$\int_0^t f(s) ds = F^T P \Phi(t).$$

The integration of the BPF vector $\Phi(t)$, with $t \in [0, 1)$, via the Itô integral can be executed by [6]

$$\int_0^t \Phi(\tau)dB(\tau) = P_S\Phi(t), t \in [0, 1) \quad (5)$$

Hence, the Itô integral of every function $f(t) \in L^2[0, 1)$ can be represented as

$$\int_0^t f(s)dB(s) = F^T P_S\Phi(t).$$

The Next theorem elucidates a correlation between the Walsh function and the block pulse function.

Theorem 1. [12] Let the m -set of Walsh function and BPF vectors be $W(t)$ and $\Phi(t)$ respectively. Then the BPF vectors $\Phi(t)$ can be used to approximate $W(t)$ as $W(t) = T_W\Phi(t)$, $m = 2^k$, and $k = 0, 1, \dots$, where $T_W = [c_{ij}]_{m \times m}$, $c_{ij} = w_i(\eta_j)$, for some $\eta_j = (\frac{j}{m}, \frac{j+1}{m})$ and $i, j = 0, 1, 2, \dots, m-1$.

One can see that [7]

$$T_W T_W^T = mI \text{ and } T_W^T = T_W$$

which implies that $\Phi(t) = \frac{1}{m}T_W W(t)$.

Lemma 1. [12][Integration of Walsh function] Suppose that $W(t)$ is a Walsh function vector, then the integral of $W(t)$ w.r.t. t is given by

$\int_0^t W(s)ds = \wedge W(t)$, where $\wedge = \frac{1}{m}T_W P T_W$ and

$$P = \frac{1}{h} \begin{bmatrix} 1 & 2 & 2 & \dots & 2 \\ 0 & 1 & 2 & \dots & 2 \\ \vdots & \vdots & \vdots & \ddots & \vdots \\ 0 & 0 & 0 & \dots & 1 \end{bmatrix}$$

Lemma 2. [12][Stochastic integration of Walsh function] Suppose that $W(t)$ is a Walsh function vector, then the Itô integral of $W(t)$ is given by

$\int_0^t W(s)dB(s) = \wedge_S W(t)$, where $\wedge_S = \frac{1}{m}T_W P_S T_W$ and

$$P_S = \begin{bmatrix} B(\frac{h}{2}) & B(h) & \dots & B(h) \\ 0 & B(\frac{3h}{2}) - B(h) & \dots & B(2h) - B(h) \\ \vdots & \vdots & \ddots & \vdots \\ 0 & 0 & \dots & B(\frac{(2m-1)h}{2}) - B((m-1)h) \end{bmatrix}.$$

4. Numerical method for NLSVIE

Let us consider the NLSVIE as

$$x(t) = x_0 + \int_0^t k_1(s, t)\beta(x(s))ds + \int_0^t k_2(s, t)\sigma(x(s))dB(s) \quad (6)$$

where $x(t)$, $k_1(s, t)$, $k_2(s, t)$ for $s, t \in [0, T)$, represent the stochastic processes based on the same probability space (Ω, F, P) and $x(t)$ is unknown. Here $B(t)$ is Brownian motion [1, 2] and $\int_0^t k_2(s, t)x(s)dB(s)$ is the Itô integral.

Let $z_1(t) = \beta(x(s))$ and $z_2(t) = \sigma(x(s))$ which implies,

$$x(t) = x_0 + \int_0^t k_1(s, t)z_1(t)ds + \int_0^t k_2(s, t)z_2(t)dB(s).$$

We can approximate $z_1(t)$, $z_2(t)$, $k_1(s, t)$, $k_2(s, t)$ for $s, t \in [0, T)$ as

$$z_\eta(t) \simeq Z_\eta^T T_W W(t), \quad \eta = 1, 2, \quad (7)$$

where $Z_\eta = [c_0 \ c_1 \ c_2 \ \dots \ c_{m-1}]^T$ and $c_i = \int_{ih}^{(i+1)h} z_\eta(s) ds$.
Similarly, for $\gamma = 1, 2$

$$k_\gamma(s, t) \simeq W^T(s) T_W K_\gamma T_W W(t) = W^T(t) T_W K_\gamma^T T_W W(s) \quad (8)$$

where $K_\gamma = [k_{ij}]_{m \times m}$, $k_{ij} = \int_{ih}^{(i+1)h} \int_{jh}^{(j+1)h} k_\gamma(s, t) dt ds$.

Assume that

$$x(t) \simeq X^T T_W W(t), \quad (9)$$

where $X = [x_0 \ x_1 \ x_2 \ \dots \ x_{m-1}]^T$ and $x_i = \int_{ih}^{(i+1)h} x(s) ds$. Replacing (7), (9) and (8) in (24) leads to

$$\begin{aligned} X^T T_W W(t) &\simeq x_0 + \int_0^t W^T(t) T_W K_1^T T_W W(s) W^T(s) T_W Z_1 ds \\ &\quad + \int_0^t W^T(t) T_W K_2^T T_W W(s) W^T(s) T_W Z_2 dB(s) \\ &= x_0 + W^T(t) T_W K_1^T T_W \int_0^t W(s) W^T(s) T_W Z_1 ds \\ &\quad + W^T(t) T_W K_2^T T_W \int_0^t W(s) W^T(s) T_W Z_2 dB(s) \end{aligned} \quad (10)$$

Now

$$\int_0^t W(s) W^T(s) T_W Z_1 ds = T_W \tilde{Z}_1 P T_W W(t) \quad (11)$$

Similarly,

$$\int_0^t W(s) W^T(s) T_W Z_2 dB(s) = T_W \tilde{Z}_2 P_S T_W W(t) \quad (12)$$

Inserting (11) and (12) in (10) we obtain,

$$\begin{aligned} X^T T_W W(t) &= x_0 + m W^T(t) T_W K_1^T \tilde{Z}_1 P T_W W(t) \\ &\quad + m W^T(t) T_W K_2^T \tilde{Z}_2 P_S T_W W(t) \\ &= x_0 + W^T(t) T_W H_1 T_W W(t) + W^T(t) T_W H_2 T_W W(t) \\ &= x_0 + m \hat{H}_1^T T_W W(t) + m \hat{H}_2^T T_W W(t) \end{aligned}$$

i.e.,

$$\left(X^T - m \hat{H}_1^T - m \hat{H}_2^T \right) T_W W(t) = x_0 \quad (13)$$

and,

$$\begin{aligned} Z_1^T T_W W(t) &= \beta(x_0 + m \hat{H}_1^T T_W W(t) + m \hat{H}_2^T T_W W(t)) \\ Z_2^T T_W W(t) &= \sigma(x_0 + m \hat{H}_1^T T_W W(t) + m \hat{H}_2^T T_W W(t)) \end{aligned} \quad (14)$$

in which $H_1 = m K_1^T \tilde{Z}_1 P$, $H_2 = m K_2^T \tilde{Z}_2 P_S$ and \hat{H}_i denotes the m -vector with elements equal to the diagonal entries of H_i .

To calculate Z_1 and Z_2 , we collocate the aforementioned equation (14) at $t_j = \frac{2j+1}{2m}$ for $j = 0, 1, \dots, m-1$ and solve the following system

$$\begin{aligned} Z_1^T T_W W(t_j) &= \beta(x_0 + m \hat{H}_1^T T_W W(t_j) + m \hat{H}_2^T T_W W(t_j)) \\ Z_2^T T_W W(t_j) &= \sigma(x_0 + m \hat{H}_1^T T_W W(t_j) + m \hat{H}_2^T T_W W(t_j)) \end{aligned} \quad (15)$$

5. Error Analysis

This section focuses on analyzing the discrepancy between the approximate and exact solutions of the stochastic Volterra integral equation. Prior to commencing the analysis, we define the notation $E(|X|^2)^{\frac{1}{2}} = \|X\|_2$.

Theorem 2. [12] If $f \in L^2[0, 1)$ and fulfills the Lipschitz condition with a Lipschitz constant C , then the 2-norm of $e_m(t)$ is $\mathcal{O}(h)$, where $e_m(t) = |f(t) - \sum_{i=0}^{m-1} c_i w_i(t)|$ and $c_i = \int_0^1 f(s) w_i(s) ds$.

Theorem 3. [12] Assume that $k \in L^2([0, 1) \times [0, 1))$ fulfills the Lipschitz condition with Lipschitz constant L . If $k_m(x, y) = \sum_{i=0}^{m-1} \sum_{j=0}^{m-1} c_{ij} w_i(x) w_j(y)$, $c_{ij} = \int_0^1 \int_0^1 k(s, t) w_i(s) w_j(t) dt ds$, then $\|e_m(x, y)\|_2 = \mathcal{O}(h)$, where $|e_m(x, y)| = |k(x, y) - k_m(x, y)|$.

Theorem 4. Assume that $x_m(t)$ be the approximated solution of the NLSIE (24). If

- $f \in L^2[0, 1)$, $k_1(s, t)$ and $k_2(s, t) \in L^2([0, 1) \times [0, 1))$ fulfills the Lipschitz condition with Lipschitz constants with Lipschitz constants C , L_1 and L_2 respectively
- $|k_1(s, t)| \leq \rho_1$, $|k_2(s, t)| \leq \rho_2$, $|\beta(x(t))| \leq \zeta_1$ and $|\sigma(x(t))| \leq \zeta_2$, and
- for $\eta_1, \eta_2 \geq 0$, $|\beta(x(t)) - \beta(x_m(t))| \leq \eta_1 |x(t) - x_m(t)|$, $|\sigma(x(t)) - \sigma(x_m(t))| \leq \eta_2 |x(t) - x_m(t)|$.

Then, we have $\|x(t) - x_m(t)\|_2^2 = \mathcal{O}(h^2)$.

Proof Consider the Volterra integral equation (24) and let $x_m(t)$ be the approximation of the solution obtained using the Walsh function. Then, we have

$$\begin{aligned} x(t) - x_m(t) &= f(t) - f_m(t) \\ &+ \int_0^t (k_1(s, t)\beta(x(s)) - k_{1m}(s, t)\beta(x_m(s))) ds \\ &+ \int_0^t (k_2(s, t)\sigma(x(s)) - k_{2m}(s, t)\sigma(x_m(s))) dB(s) \end{aligned}$$

or,

$$\begin{aligned} |x(t) - x_m(t)| &\leq |f(t) - f_m(t)| \\ &+ \left| \int_0^t (k_1(s, t)\beta(x(s)) - k_{1m}(s, t)\beta(x_m(s))) ds \right| \\ &+ \left| \int_0^t (k_2(s, t)\sigma(x(s)) - k_{2m}(s, t)\sigma(x_m(s))) dB(s) \right|. \end{aligned}$$

We know that, $(a + b + c)^2 \leq 3a^2 + 3b^2 + 3c^2$

$$\begin{aligned} |x(t) - x_m(t)|^2 &\leq 3|f(t) - f_m(t)|^2 \\ &+ 3 \left| \int_0^t (k_1(s, t)\beta(x(s)) - k_{1m}(s, t)\beta(x_m(s))) ds \right|^2 \\ &+ 3 \left| \int_0^t (k_2(s, t)\sigma(x(s)) - k_{2m}(s, t)\sigma(x_m(s))) dB(s) \right|^2. \end{aligned}$$

which implies that

$$\begin{aligned}
E(|x(t) - x_m(t)|^2) &\leq E\left(3|f(t) - f_m(t)|^2\right) \\
&+ E\left(3\left|\int_0^t (k_1(s, t)\beta(x(s)) - k_{1m}(s, t)\beta(x_m(s)))ds\right|^2\right) \\
&+ E\left(3\left|\int_0^t (k_2(s, t)\sigma(x(s)) - k_{2m}(s, t)\sigma(x_m(s)))dB(s)\right|^2\right).
\end{aligned} \tag{16}$$

Suppose,

$$I_1 = E\left(3\left|\int_0^t (k_1(s, t)\beta(x(s)) - k_{1m}(s, t)\beta(x_m(s)))ds\right|^2\right)$$

and

$$I_2 = E\left(3\left|\int_0^t (k_2(s, t)\sigma(x(s)) - k_{2m}(s, t)\sigma(x_m(s)))dB(s)\right|^2\right).$$

Applying the Theorem 2 in inequality (16) results

$$E(|x(t) - x_m(t)|^2) \leq C^2h^2 + I_1 + I_2 \tag{17}$$

Now,

$$\begin{aligned}
|k_1(s, t)\beta(x(s)) - k_{1m}(s, t)\beta(x_m(s))| &= |k_1(s, t)\beta(x(s)) - k_1(s, t)\beta(x_m(s)) \\
&+ k_1(s, t)\beta(x_m(s)) - k_{1m}(s, t)\beta(x_m(s))| \\
&\leq |k_1(s, t)||\beta(x(s)) - \beta(x_m(s))| \\
&+ |k_1(s, t) - k_{1m}(s, t)||\beta(x_m(s))| \\
&= |k_1(s, t)||\beta(x(s)) - \beta(x_m(s))| \\
&+ |k_1(s, t) - k_{1m}(s, t)||\beta(x(s)) - \beta(x_m(s)) + \beta(x_m(s))| \\
&\leq |k_1(s, t)||\beta(x(s)) - \beta(x_m(s))| \\
&+ |k_1(s, t) - k_{1m}(s, t)||\beta(x(s))| \\
&+ |k_1(s, t) - k_{1m}(s, t)||\beta(x_m(s))|
\end{aligned}$$

Let $|k_1(s, t)| \leq \rho_1$, $|\beta(x(t))| \leq \zeta_1$, $|\beta(x(t)) - \beta(x_m(t))| \leq \eta_1|x(t) - x_m(t)|$ and using Theorem 3, we get

$$\begin{aligned}
|k_1(s, t)\beta(x(s)) - k_{1m}(s, t)\beta(x_m(s))| &\leq \rho_1\eta_1|x(s) - x_m(s)| \\
&+ \sqrt{2}L_1h\zeta_1 + \sqrt{2}L_1h\eta_1|x(s) - x_m(s)|
\end{aligned}$$

which arrives at

$$|k_1(s, t)\beta(x(s)) - k_{1m}(s, t)\beta(x_m(s))| \leq \sqrt{2}L_1h\zeta_1 + (\rho_1\eta_1 + \sqrt{2}L_1h\eta_1)|x(s) - x_m(s)| \tag{18}$$

which gives,

$$\begin{aligned}
I_1 &\leq E\left(3\left(\int_0^t |k_1(s, t)\beta(x(s)) - k_{1m}(s, t)\beta(x_m(s))|ds\right)^2\right) \\
&\leq E\left(3\left(\int_0^t (\sqrt{2}L_1h\zeta_1 \right. \right. \\
&\quad \left. \left. + (\rho_1\eta_1 + \sqrt{2}L_1h\eta_1)|x(s) - x_m(s)|)ds\right)^2\right)
\end{aligned}$$

In virtue of the Cauchy- Schwarz inequality, for $t > 0$ and $f \in L^2[0, t)$

$$\left| \int_0^t f(s) ds \right|^2 \leq t \int_0^t |f|^2 ds$$

this implies,

$$\begin{aligned} I_1 &\leq E \left(3 \int_0^t \left(\sqrt{2}L_1 h \zeta \right. \right. \\ &\quad \left. \left. + (\rho_1 \eta_1 + \sqrt{2}L_1 h \eta_1) |x(s) - x_m(s)| \right)^2 ds \right) \\ &\leq E \left(6 \int_0^t \left((\sqrt{2}L_1 h \zeta_1)^2 \right. \right. \\ &\quad \left. \left. + ((\rho_1 \eta_1 + \sqrt{2}L_1 h \eta_1) |x(s) - x_m(s)|)^2 \right) ds \right) \\ &\leq E \left(6(\sqrt{2}L_1 h \zeta_1)^2 \right. \\ &\quad \left. + 6(\rho_1 \eta_1 + \sqrt{2}L_1 h \eta_1)^2 \int_0^t |x(s) - x_m(s)|^2 ds \right) \end{aligned}$$

Hence,

$$\begin{aligned} I_2 &\leq 6(\sqrt{2}L_1 h \zeta_1)^2 \\ &\quad + 6(\rho_1 \eta_1 + \sqrt{2}L_1 h \eta_1)^2 \int_0^t E(|x(s) - x_m(s)|^2) ds. \end{aligned} \tag{19}$$

Now,

$$I_2 \leq E \left(3 \int_0^t \left| k_2(s, t) \sigma(x(s)) - k_{2m}(s, t) \sigma(x_m(s)) \right|^2 ds \right)$$

Let $|k_2(s, t)| \leq \rho_2$, $|\sigma(x(t))| \leq \zeta_2$, $|\sigma(x(t)) - \sigma(x_m(t))| \leq \eta_2 |x(t) - x_m(t)|$ and using Theorem 3, we get

$$|k_2(s, t) \sigma(x(s)) - k_{2m}(s, t) \sigma(x_m(s))| \leq \sqrt{2}L_2 h \zeta_2 + (\rho_2 \eta_2 + \sqrt{2}L_2 h \eta_2) |x(s) - x_m(s)|$$

$$\begin{aligned} I_2 &\leq E \left(3 \int_0^t \left(\sqrt{2}L_2 h \zeta_2 + (\rho_2 \eta_2 + \sqrt{2}L_2 h \eta_2) |x(s) - x_m(s)| \right)^2 ds \right) \\ &\leq E \left(6 \int_0^t \left((\sqrt{2}L_2 h \zeta_2)^2 + (\rho_2 \eta_2 + \sqrt{2}L_2 h \eta_2)^2 |x(s) - x_m(s)|^2 \right) ds \right) \\ &= E \left(6(\sqrt{2}L_2 h \zeta_2)^2 + 6(\rho_2 \eta_2 + \sqrt{2}L_2 h \eta_2)^2 \int_0^t |x(s) - x_m(s)|^2 ds \right) \end{aligned}$$

Hence,

$$\begin{aligned} I_2 &\leq 6(\sqrt{2}L_2 h \zeta_2)^2 \\ &\quad + 6(\rho_2 \eta_2 + \sqrt{2}L_2 h \eta_2)^2 \int_0^t E(|x(s) - x_m(s)|^2) ds \end{aligned} \tag{20}$$

Employing (19) and (20) in (17), we have

$$\begin{aligned}
E(|x(t) - x_m(t)|^2) &\leq C^2 h^2 \\
&\quad + 6(\sqrt{2}L_1 h \zeta_1)^2 \\
&\quad + 6(\rho_1 \eta_1 + \sqrt{2}L_1 h \eta_1)^2 \int_0^t E(|x(s) - x_m(s)|^2) ds \\
&\quad + 6(\sqrt{2}L_2 h \zeta_2)^2 \\
&\quad + 6(\rho_2 \eta_2 + \sqrt{2}L_2 h \eta_2)^2 \int_0^t E(|x(s) - x_m(s)|^2) ds
\end{aligned}$$

which implies that

$$\begin{aligned}
E(|x(t) - x_m(t)|^2) &\leq (C^2 h^2 + 6(\sqrt{2}L_1 h \zeta_1)^2 + 6(\sqrt{2}L_2 h \zeta_2)^2) \\
&\quad + (6(\rho_1 \eta_1 + \sqrt{2}L_1 h \eta_1)^2 + 6(\rho_2 \eta_2 + \sqrt{2}L_2 h \eta_2)^2) \int_0^t E(|x(s) - x_m(s)|^2) ds.
\end{aligned} \tag{21}$$

Let

$$\begin{aligned}
R_1 &= (C^2 h^2 + 6(\sqrt{2}L_1 h \zeta_1)^2 + 6(\sqrt{2}L_2 h \zeta_2)^2) \\
R_2 &= (6(\rho_1 \eta_1 + \sqrt{2}L_1 h \eta_1)^2 + 6(\rho_2 \eta_2 + \sqrt{2}L_2 h \eta_2)^2)
\end{aligned}$$

By using Gronwall's inequality, we have

$$E(|x(t) - x_m(t)|^2) \leq R_1 \exp\left(\int_0^t R_2 ds\right). \tag{22}$$

which implies that,

$$\|x(t) - x_m(t)\|_2^2 = E(|x(t) - x_m(t)|^2) \leq R_1 e^{R_2 t} = O(h^2) \tag{23}$$

6. Numerical Examples

This section employs the proposed method to solve the NLSVIE. Two numerical examples are given to demonstrate the convergence of the method by comparing the approximate and analytical results. To measure the error between the two solutions, the infinity norm of the error E is defined as $\|E\|_\infty = \max_{1 \leq i \leq m} |X_i - Y_i|$, where X_i and Y_i are the Walsh coefficients of the exact and approximate solutions, respectively. The number of iterations for each example is denoted as n , while the mean and standard deviation of the error E are represented as \bar{x}_E and s_E , respectively. All computations are performed using Matlab 2013(a).

Example 1. [1] Let us consider the NLSVIE

$$x(t) = x_0 - \frac{a^2}{2} \int_0^t \tanh(x(s)) \operatorname{sech}^2(x(s)) ds + a \int_0^t \operatorname{sech}(x(s)) dB(s)$$

where, $x_0 = 0$ and $a = \frac{1}{30}$ and $x(t)$ represents the unknown stochastic process based on the same probability space (Ω, F, P) , and $B(t)$ is a Brownian motion process. The exact solution is given by $x(t) = \sinh^{-1}(aB(t) + \sinh(x_0))$.

Table 1 reports \bar{x}_E and s_E errors as well as interval of confidence for mean error with $m = 16$ and 50 iterations. Figure 1 displays the numerical and exact solutions with $m = 32$ and $m = 64$. Figure 2 shows the behavior of error solutions with $m = 16$, $m = 32$, and $n = 50$. Table 2 represents \bar{x}_E and s_E errors as well as interval of confidence for mean error with $m = 32$ and 50 iterations.

Table 1: \bar{x}_E and s_E errors as well as interval of confidence for mean error in Example 1 with $m = 16$ and 50 iterations.

| t | \bar{x}_E | s_E | 95% interval of confidence for error mean | |
|-----|-------------------------|-------------------------|-------------------------------------------|-------------------------|
| | | | Lower | Upper |
| 0.1 | 0.0073×10^{-5} | 0.0137×10^{-5} | 0.0348×10^{-6} | 0.0111×10^{-5} |
| 0.3 | 0.0330×10^{-5} | 0.1151×10^{-5} | 0.0109×10^{-6} | 0.0649×10^{-5} |
| 0.5 | 0.0900×10^{-5} | 0.3352×10^{-5} | 0.0290×10^{-6} | 0.1829×10^{-5} |
| 0.7 | 0.1402×10^{-5} | 0.4698×10^{-5} | 0.0995×10^{-6} | 0.2704×10^{-5} |
| 0.9 | 0.1939×10^{-5} | 0.6806×10^{-5} | 0.0519×10^{-6} | 0.3825×10^{-5} |

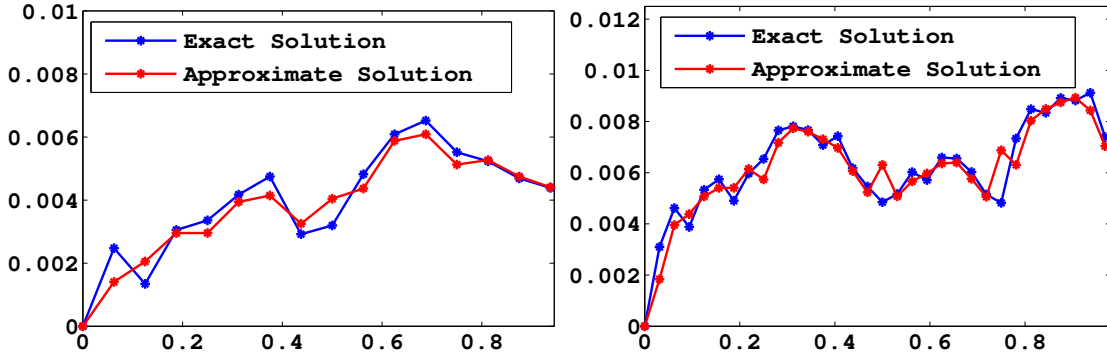


Figure 1: The numerical and exact solutions of Example 1 with $m = 32$ and $m = 64$.

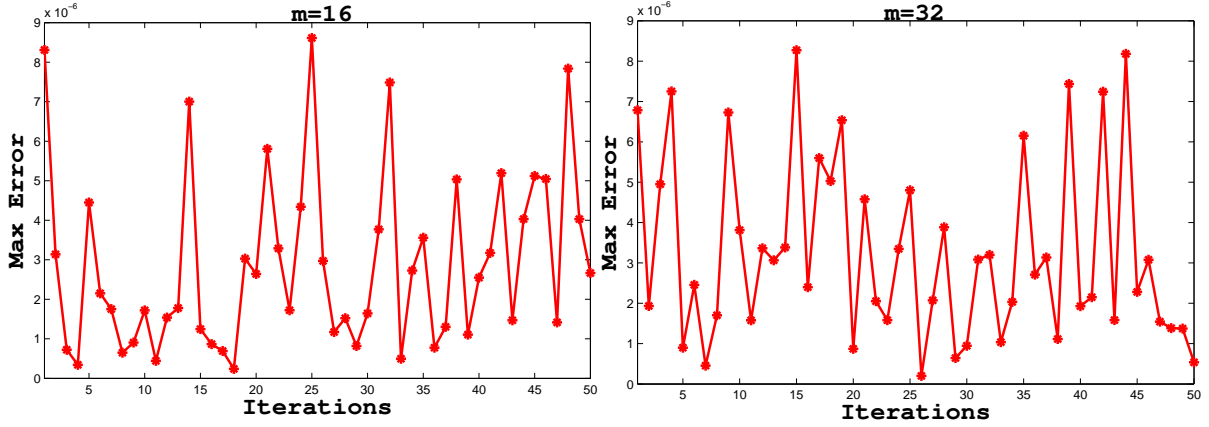


Figure 2: The behavior of error solutions in Example 1 with $m = 16, m = 32$, and $n = 50$

Table 2: \bar{x}_E and s_E errors as well as interval of confidence for mean error in Example 1 with $m = 32$ and 50 iterations.

| t | \bar{x}_E | s_E | 95% interval of confidence for error mean | |
|-----|-------------------------|-------------------------|-------------------------------------------|-------------------------|
| | | | Lower | Upper |
| 0.1 | 0.0192×10^{-5} | 0.0223×10^{-5} | 0.0130×10^{-5} | 0.0254×10^{-5} |
| 0.3 | 0.0809×10^{-5} | 0.1477×10^{-5} | 0.0400×10^{-5} | 0.1219×10^{-5} |
| 0.5 | 0.1577×10^{-5} | 0.3446×10^{-5} | 0.0621×10^{-5} | 0.2532×10^{-5} |
| 0.7 | 0.2262×10^{-5} | 0.4336×10^{-5} | 0.1061×10^{-5} | 0.3464×10^{-5} |
| 0.9 | 0.2992×10^{-5} | 0.5677×10^{-5} | 0.1418×10^{-5} | 0.4565×10^{-5} |

Example 2. [1] Consider the NLSVIE

$$x(t) = x_0 - a^2 \int_0^t x(s)(1 - x^2(s))ds + a \int_0^t (1 - x^2(s))dB(s) \quad (24)$$

where, $x_0 = \frac{1}{10}$ and $a = \frac{1}{30}$ and $x(t)$ represents the unknown stochastic process based on the same probability space (Ω, F, P) , and $B(t)$ is a Brownian motion process. The exact solution is given by $x(t) = \tanh(aB(t) + \tanh^{-1}(x_0))$.

Table 3 displays \bar{x}_E and s_E errors as well as interval of confidence for mean error with $m = 16$ and 50 iterations. Table 4 presents \bar{x}_E and s_E errors as well as interval of confidence for mean error with $m = 32$ and 50 iterations. Figure 3 shows the numerical and exact solutions with $m = 16$ and $m = 632$.

Table 3: \bar{x}_E and s_E error as well as interval of confidence for mean error in Example 2 with $m = 16$ and 50 iterations.

| t | \bar{x}_E | s_E | 95% interval of confidence for error mean. | |
|-----|-------------------------|-------------------------|--------------------------------------------|-------------------------|
| | | | Lower | Upper |
| 0.1 | 0.1029×10^{-4} | 0.0045×10^{-4} | 0.1016×10^{-4} | 0.0104×10^{-3} |
| 0.3 | 0.3070×10^{-4} | 0.0284×10^{-4} | 0.2992×10^{-4} | 0.0315×10^{-3} |
| 0.5 | 0.5373×10^{-4} | 0.0761×10^{-4} | 0.5163×10^{-4} | 0.0558×10^{-3} |
| 0.7 | 0.7689×10^{-4} | 0.1193×10^{-4} | 0.7358×10^{-4} | 0.0802×10^{-3} |
| 0.9 | 0.9666×10^{-4} | 0.1706×10^{-4} | 0.9193×10^{-4} | 0.1014×10^{-3} |

Table 4: \bar{x}_E and s_E errors as well as interval of confidence for mean error in Example 2 with $m = 32$ and 50 iterations.

| t | \bar{x}_E | s_E | 95% interval of confidence for error mean | |
|-----|-------------------------|-------------------------|-------------------------------------------|-------------------------|
| | | | Lower | Upper |
| 0.1 | 0.1184×10^{-4} | 0.0064×10^{-4} | 0.1156×10^{-4} | 0.0121×10^{-3} |
| 0.3 | 0.3161×10^{-4} | 0.0281×10^{-4} | 0.3038×10^{-4} | 0.0328×10^{-3} |
| 0.5 | 0.5215×10^{-4} | 0.0832×10^{-4} | 0.4850×10^{-4} | 0.0557×10^{-3} |
| 0.7 | 0.7284×10^{-4} | 0.1288×10^{-4} | 0.6719×10^{-4} | 0.0784×10^{-3} |
| 0.9 | 0.9216×10^{-4} | 0.1893×10^{-4} | 0.8387×10^{-4} | 0.1004×10^{-3} |

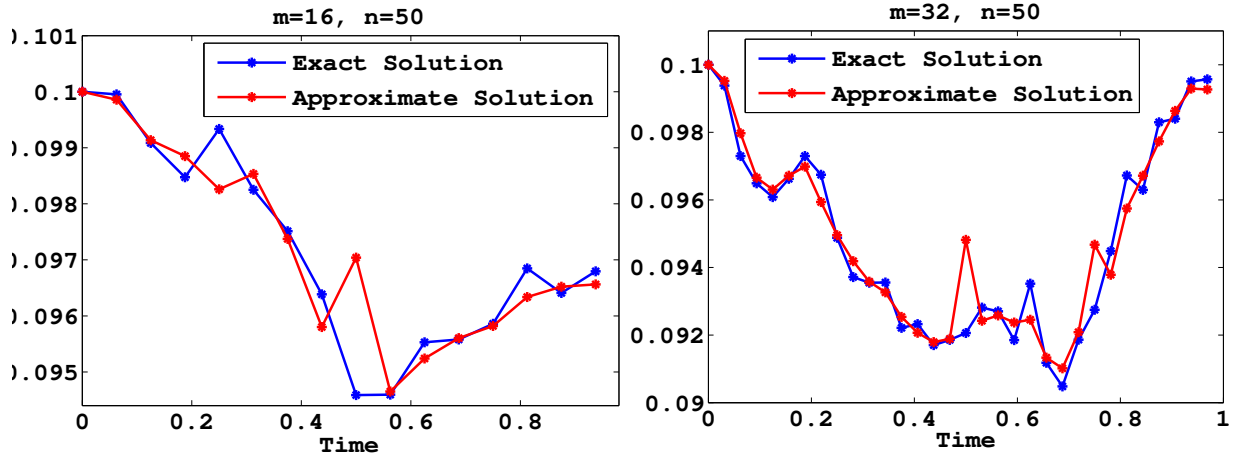


Figure 3: The numerical and exact solutions of Example 2 with $m = 16$ and $m = 32$.

7. Conclusion

This paper implemented the proposed numerical approach based on the Walsh function to solve the integral equation, which transforms the problem into a set of algebraic equations. These equations are then solved to obtain an approximation of the solution. Through convergence and error analysis, the method's order of

convergence is found to be $\mathcal{O}(h)$. The method was applied to numerical examples with known exact solutions in the final section, and the results are presented in tables and figures. These results demonstrated that the method is highly accurate and efficient, with high precision achievable using a limited number of basis functions. Increasing the number of basis functions reduces absolute errors. Additionally, the method can be adapted to solve non-linear stochastic integral equations with fractional Brownian motion.

References

References

- [1] P.E. Kloeden, E. Platen, Numerical Solution of Stochastic Differential Equations, in: Applications of Mathematics, Springer-Verlag, Berlin, 1999.
- [2] B. Oksendal, Stochastic Differential Equations, fifth ed., in: An Introduction with Applications, Springer-Verlag, New York, 1998.
- [3] J. L. Walsh, A closed set of normal orthogonal functions, Amer. J. Math. vol. 55 (1923) pp. 5-24.
- [4] G. Prasada Rao, Piecewise Constant Orthogonal Functions and Their Application to Systems and Control, Springer, Berlin, 1983.
- [5] Saeed Hatamzadeh-Varmazyar, Zahra Masouri, Esmail Babolian, Numerical method for solving arbitrary linear differential equations using a set of orthogonal basis functions and operational matrix, Applied Mathematical Modelling 40 (2016) 233–253.
- [6] K. Maleknejad, M. Khodabin, M. Rostami, Numerical solution of stochastic Volterra integral equations by a stochastic operational matrix based on block pulse functions, Mathematical and Computer Modelling, Mathematical and Computer Modelling 55 (2012) 791–800.
- [7] C. F. Cheng, Y. Tsay, T. T. Wu, Walsh operational matrices for fractional calculus and their application to distributed systems, Journal of The Franklin Institute-engineering and Applied Mathematics(1997).
- [8] B. Golubov, A. Efimov, V. Skvortsov, Walsh Series and Transforms Theory and Applications.
- [9] M. Asgari, F. H. Shekarabi, Numerical solution of nonlinear stochastic differential equations using the block pulse operational matrices. Math Sci 7, 47 (2013).
- [10] R. Zeghdane, Numerical approach for solving nonlinear stochastic Itô-Volterra integral equations using shifted Legendre polynomials, International Journal of Dynamical Systems and Differential Equations 11.1 (2021): 69-88.
- [11] J. Wu, G. Jiang, X. Sang, Numerical solution of nonlinear stochastic Itô-Volterra integral equations based on Haar wavelets. Adv Differ Equ 2019, 503 (2019).
- [12] Paikaray P. P., Beuria S., Parida N. Ch., Numerical approximation of p-dimensional stochastic Volterra integral equation using Walsh function. J Math Comput SCI-JM.(2023); 31(4):448–460